

Original Articles

Histological study of the unsintered carbonate containing apatite porous body in beagle dog dorsal muscle

SHIBATSUJI ATSUSHI, KANAYAMA KEIICHI, MUKAI KEISUKE, OTARI SYUHEI,
MORINAGA HIROTUGU, KITAGO MITSUNOBU, HASEGAWA TORU, KIMURA YOKO,
TAKEUCHI HIROKO, DOI YUTAKA, SHIBUTANI TOSHIAKI

Bone apatite is not composed of pure hydroxyapatite (HAp), but contains calcium, phosphoric acid, hydroxyl groups and is substituted with many ions. The difference between bone apatite and HAp is the absence of carbonate ions in HAp. Recently, synthetic carbonated apatite (sCA) has been proposed as a substitute bone material, showing both excellent biocompatibility and bioabsorbability.

Recently, we have newly developed and reported unsintered carbonate-containing apatite (usCA), which is synthesized from dibasic calcium phosphate dihydrate (DCPD). In this study, we investigated the histological changes in usCA containing tissue following implantation in the dorsal muscle of beagle dogs in comparison with sCA and β -tricalcium phosphate (TCP). Eighteen male beagle dogs received an incision in three vertical positions, and the experimental materials were embedded in an envelope formed in the dorsal muscle. Each sample was photographed using a micro computed tomography (μ CT) analyzer. Following removal of the samples, tissue sections were stained with hematoxylin and eosin, alkaline phosphatase (ALP) and tartrate-resistant acid phosphatase (TRAP). Analysis with μ CT showed that the usCA group showed a significantly higher absorption rate than the sCA and β -TCP groups at 3 and 6 months. usCA showed superior tissue compatibility, ectopic bone formation and absorbability. Thus, this material appears to be suited for clinical applications.

Key words: Carbonate containing apatite, Tricalcium phosphate, Beagle dog, Histological study

Introduction

Bone regeneration and restoration of biological functions are performed in regenerative medicine using biomaterial fillers^{1,3)}. The use of autogenous bone grafting is considered the gold standard for bone regeneration, however the supply of materials is limited. In addition, the use of allogeneic bone may be complicated by the development of infectious diseases^{1,5)}. A variety of artificial bones have been developed as substitutes of autologous bone and allogeneic bone. At present, tricalcium phosphate (TCP), hydroxyapatite (HAp), and sintered carbonate-containing apatite (sCA) are used as scaffold-type bone substitute materials⁶⁾. HAp is similar to the inorganic components of bone and has excellent biocompatibility, but shows low absorption *in vivo*¹⁾. Moreover, HAp persists over the long term and causes infections. On the other hand, beta-tricalcium phosphate (β -TCP) is osteoconductive, but is not naturally present in bone¹; it is reported to be phagocytosed by

macrophages⁶⁾. From the viewpoint of biocompatibility, a material comparable to HAp and absorbed by osteoclasts is thought to be an ideal scaffold-type prosthetic bone material^{1,6)}.

Bone apatite is not purely composed of HAp, containing calcium, phosphoric acid, and hydroxyl groups and is substituted with many ions^{1,6)}. The difference between bone apatite and HAp is the absence of carbonate ions in HAp, with bone apatite containing about 5 to 8% carbonate ions.

Recently, sCA has been suggested as a substitute bone material, showing both excellent biocompatibility and bioabsorbability^{1,6)}. We have newly developed and reported unsintered carbonate-containing apatite (usCA) synthesized from dibasic calcium phosphate dihydrate (DCPD)⁶⁾. In this study, we investigated histological changes in usCA containing tissues following implantation in the dorsal muscle of beagle dogs in comparison with sCA and β -TCP.

Materials and methods

Experimental materials and animals

The following experimental materials were used: usCA (porosity 53%), sCA (porosity 56%, carbonic acid content, 9.4%) and β -TCP (OSferion®, Olympus, Tokyo, OS). All materials were trimmed to a cylindrical shape, 8mm in diameter and 10 mm in length.

Eighteen male beagle dogs aged 1.5 to 8years old and weighing 10 to 12kg were divided into six groups of three dogs each. This experiment was conducted according to the guidelines for Asahi University laboratory animals.

A combination of general and local anesthesia was employed; 0.05mg/kg of xylazine hydrochloride (secretal 2% injection, Bayer, Tokyo) was injected intramuscularly along with 0.4ml/kg sodium pentobarbital (Somnopentyl®, Kyoritsu Seiyaku, Tokyo), while local anesthesia was performed using lidocaine hydrochloride (Xylocaine Cartridge®, Dentspruit Sanki, Tokyo) containing epinephrine. An envelope-like flap was made on the dorsal surface of the beagles using a scalpel, and the experimental materials were embedded. The muscle was sutured with absorbable thread (Vicryl Rapid®, Matsukaze, Kyoto), and the epidermis was sutured with a nonabsorbable thread (Softrech®, GC, Tokyo). Following the surgery, 0.5g of the antimicrobial agent coixin (cephalothin sodium, Higashi Pharmaceutical, Tokyo) was injected intramuscularly daily for 3days. Assessments were performed at 3 and 6months post-implantation. At the end of each observation period, tissues containing the samples and muscle were removed and fixed with 4% neutral paraformaldehyde.

μ CT analysis

Individual samples were analyzed using a μ CT analyzer (Scan Xmate-RB 090 SS 150; Comscan) with a tube voltage of 90 KV, tube current of 89 μ A, tube power of 8W, and magnification of 7X. Three dimensional (3D) images were constructed using the 3D image analysis software (3D-BON, RATOC, Tokyo) and the volume of the porous body was obtained by standardizing the BMD value. The porosity rate (volume of extracted porous material / volume of known porous material) was calculated from the absorptivity of the porous material (volume of known porous material - volume of extracted porous material / volume of known porous material) and used to compare the absorptivity of porous bodies. The data was subjected to one-way analysis of variance, and multiple comparisons were performed using Tukey's method.

Tissue specimen preparation and observation

The fixed tissues were decalcified with a 10% EDTA (pH 7.4) solution. After decalcification, the samples were embedded in paraffin and 4 μ m sections were cut. The tissue sections were stained with hematoxylin and eosin (H&E) solution, alkaline phosphatase (ALP) and tartrate-resistant acid phosphatase (TRAP)⁷, and subsequently imaged using light microscopy.

Results

μ CT Analysis

Absorbency of Porous Bodies

μ CT imaging was used to calculate the porosity rate (Fig. 1), which was $92.7 \pm 6.1\%$ in the sCA group, $65.8 \pm 5.7\%$ in the β -TCP group, $18.1 \pm 7.8\%$ in the usCA group after 3months. After 6months, the porosity rate was $81.4 \pm 5.9\%$ in the sCA group, $55.9 \pm 7.4\%$ in the OS group, $5.8 \pm 8.5\%$ in the usCA group. Thus, the absorption rates were $7.28 \pm 6.1\%$ in the sCA group, $34.2 \pm 5.7\%$ in the β -TCP group, and $81.9 \pm 7.8\%$ in the usCA group after 3 months. After 6 months, it was $18.6 \pm 5.9\%$ in sCA group, $44.1 \pm 7.4\%$ in β -TCP group, $94.2 \pm 8.5\%$ in usCA group. At 3months, the usCA group showed a significantly higher absorption rate than the sCA and β -TCP groups ($p < 0.05$). At 6months, the usCA group showed a significantly higher absorption rate than the sCA group and β -TCP group at 3months ($p < 0.05$).

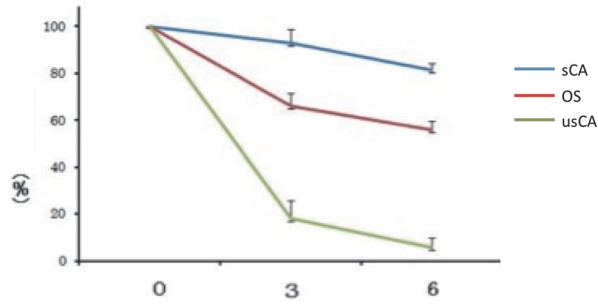


Fig.1 μ CT analysis of porous body absorbancy

Histological findings

1) usCA group

At 3months after implantation, fibrous tissue was observed around the porous body, and vigorous new bone growth occurred inside the porous body (Fig. 2-a). Osteoclasts, which are TRAP-positive and multinucleated giant cells, were observed on the surface of newly formed bone and on the surface in contact with usCA (Fig. 2-b, c). The spherical or cuboidal osteoblast cells with basophilic cytoplasm formed a bone matrix that was well-suited for eosin and osteoclasts were observed to be in contact with newly formed bone (Fig. 2-d). ALP staining showed ALP activity in the presence of osteoblast-like cells (Fig. 2-e).

At 6months post-implantation, newly formed bone was observed inside the porous body as was observed in the usCA group at 3months following implantation (Fig. 3-a). A large number of TRAP-positive cells were present on the surface of newly formed and porous bodies (Fig. 3-b). The arrangement of cuboid osteoblast-like cells is seen on the surface of newly formed structures (Fig. 3-c), and persistent bone formation can be observed.

2) β -TCP group

Newly formed bone was found inside and around the porous body at 3months post-implantation (Fig. 4-a). The formation of TRAP-positive osteoclasts and bone matrix

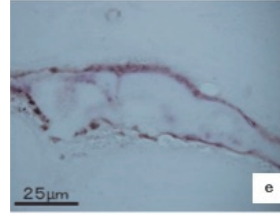
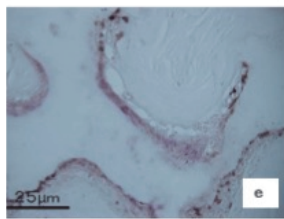
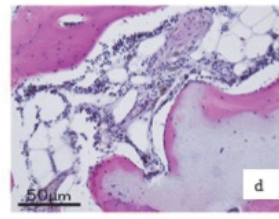
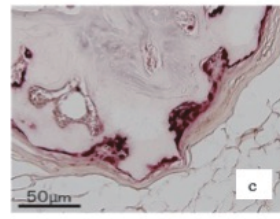
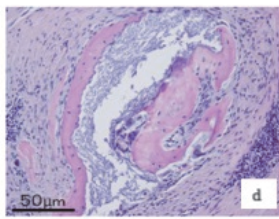
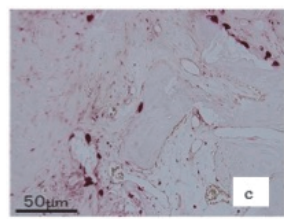
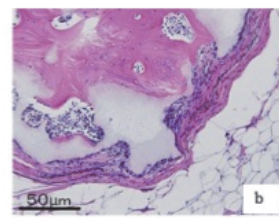
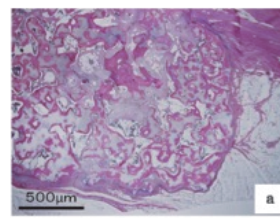
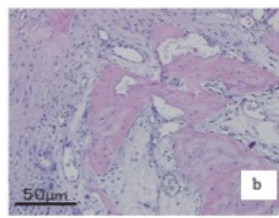
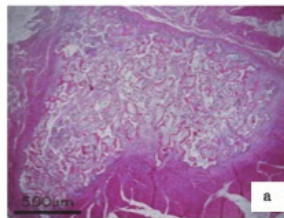


Fig.2 Histological observations at 3 months post-implantation of usCA
a, b, d HE staining, d TRAP staining, e ALP staining

Fig.4 Histological observations at 3 months post-implantation of β -TCP
a, b, d HE staining, d TRAP staining, e ALP staining

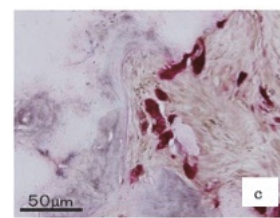
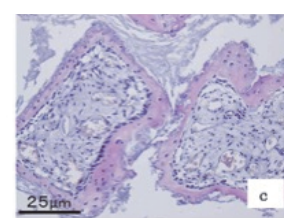
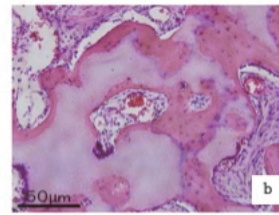
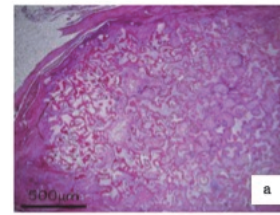
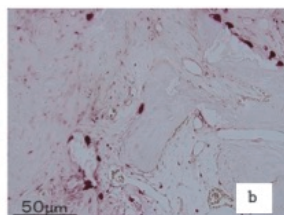
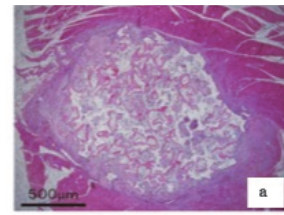


Fig.3 Histological observations at 6 months post-implantation of usCA
a, c HE staining, b TRAP staining

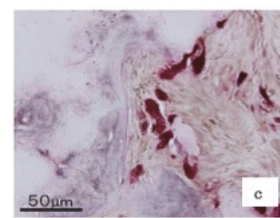


Fig.5 Histological observations at 6 months post-implantation of β -TCP
a, c HE staining, b TRAP staining

was observed at sites in contact with β -TCP (Fig. 4-b, c) (Fig. 5-a, b, c). Bone marrow tissue was found in the newly formed structures (Fig. 4-d) and ALP staining / activity was observed on their surface (Fig. 4-e).

3) sCA group

At 3months post-implantation, the pore size expanded, absorbability was confirmed, and new bone formation was observed around the porous body (Fig. 6-a). Many

osteoclasts, which are TRAP-positive and multinucleated large cells, appeared in contact with sCA and were present between the sCA and new bone (Fig. 6-b, c). In addition, numerous osteoblast-like cells were aligned along the substrate surface of newly formed bone (Fig. 6-d). ALP staining also showed ALP activity on the surface of newly formed bone (Fig. 6-e). At 6months post-implantation, the formation and absorption of the new bone was greater than that at 3months (Fig. 7-a, b, c)

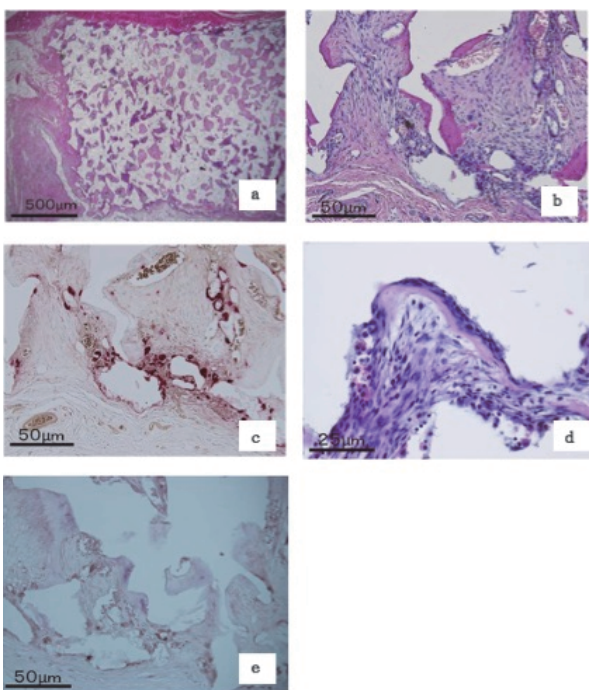


Fig.6 Histological observations at 3 months post-implantation of sCA
a, b, d HE staining, d TRAP staining, e ALP staining

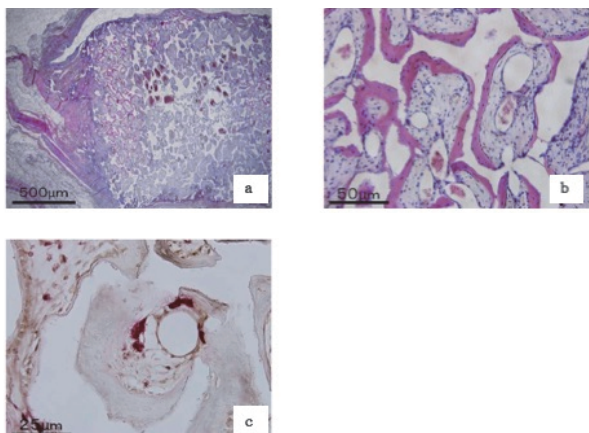


Fig.7 Histological observations at 6 months post-implantation of sCA
a, c HE staining, b TRAP staining

Discussion

There are numerous reports on bone regeneration¹⁻⁶. Calcium phosphate bone substitute materials were not thought to have osteoinductive ability; however, it was reported that bone formation occurs in 3months when HAP is implanted in dog muscle²⁻⁵. It has been reported that the osteoinduction phenomenon is observed only in materials having a macropore structure for bone induction of the calcium phosphate type bone substitute material¹⁻⁵. In addition, it is often seen in dogs and pigs

with differences due to animals, but hard to observe in rats, mice, rabbits¹⁻⁵.

It has been reported that carbonate apatite sintered bodies have excellent bioabsorbability⁸. The absorption of apatite *in vivo* is thought to be caused by the acid produced by osteoclasts^{8,9}. The mechanism of the osteoinductive potential of the calcium phosphate porous body involves the elution of calcium and phosphate ions from structures that are easily dissolved, with a subsequent increase in endogenous BMP concentrations on the surface of the porous body, and osteoblast cell differentiation¹⁰⁻¹². This study demonstrates that absorption of the porous body and ectopic bone formation is accompanied by osteoclasts and osteoblast-like cells, which was observed in all groups at 3months and 6months post-implantation. In addition, usCA exhibited excellent absorbability. Since usCA has a large carbonic acid content compared to sCA, is not sintered and has low crystallinity, its physicochemical stability decreases if carbonate ions are substituted in the apatite lattice. This is in agreement with the theory that physicochemical stability decreases when carbonate ions are substituted in the apatite lattice, and apatite is dissolved by acids produced by osteoclasts. Thus, usCA showed superior tissue compatibility, ectopic bone formation and superior absorbability, and clinical utilization of usCA is anticipated.

Conclusion

We investigated ectopic bone formation by implanting usCA, β -TCP, sCA in the muscle of beagle dogs. The following findings were obtained.

1. Ectopic bone formation was observed in all porous bodies.
2. The novel porous body was found to be inductive and showed superior absorptivity to the existing porous body and was thus suggested to be an effective option for clinical application as a scaffolding material.

There is no COI to disclose

References

- 1 Rafieerad AR, Ashra MR, Mahmoodian R, Bushroa AR. Surface characterization and corrosion behavior of calcium phosphate-base composite layer on titanium and its alloys via plasma electrolytic oxidation: A review paper. Mater Sci Eng C Mater Biol Appl. 1; 57: doi: 10.1016/j.msec.2015.07.058. Epub 2015 397-413.
- 2 Mastogiacomo M., Scaglione S., Martinetti, R.. Role of Scaffold Internal Structure on *in vivo* Bone Formation in Macroporous Calcium Phosphate Bioceramics, Biomaterials 2006; 27: 3230-3237.

- 3 Schnettler, R., Alt, V., Dingeldein, E.. Bone Ingrowth in bFGF-Coated Hydroxyapatite Ceramic Implants, *Biomaterials* 2003; 24: 4603–4608.
 - 4 Ruhé, P.Q., Kroese-Deutman, H.C., Wolke, J.G.C., Spaunwen, P.H.N., Jansen, J.A. Bone Inductive Properties of rhBMP-2 Loaded Porous Calcium Phosphate Cement Implants in Cranial Defects in Rabbits, *Biomaterials* 2004; 25: 2123–2132.
 - 5 Niedhaet, C., Maus, U., Miltner, O., Gräber, H.G., Niethard, F.U., Siebert, C.H. The Effect of Basic Fibroblast Growth Factor on Bone Regeneration when Released from a Novel in situ Setting Tricalcium Phosphate Cement, *J. Biomed. Mater. Res.* 2004; 69: 680–685.
 - 6 Shibatsui A, Kanayama K, Mukai K, Kitago M, Yasuda T, Kimura Y, Takeuchi H, Doi Y, Shibutani T. Study on preparation method of novel carbonate-containing apatite porous body. *J. Gifu Dent.* 2017.
 - 7 Shibutani T, Tsukada E, Murahashi Y, Iwayama Y and Heersche J. Experimentally Induced Periodontitis in Beagle Dogs Causes Rapid Increases in Osteoclastic Resorption of Alveolar Bone. *J. Periodontology* 1997; 68: 385–391
 - 8 Doi, Y., Shibutani, T., Moriwaki, Y., Kajimoto, T., Iwayama, Y. Sintered Carbonate Apatites as Bioresorbable Bone Substitutes, *J. Biomed. Mater. Res.* 1998; 39: 603–610.
 - 9 Li S. The *Arabidopsis thaliana* TCP transcription factors: A broadening horizon beyond development. *Plant Signal Behav.* 2015; 10: e1044192. doi: 10.1080/15592324.2015.1044192.
 - 10 Ready, S.A., Razzouk, S., Rey, C. Osteoclast Adhesion and Activity on Synthetic Hydroxyapatite, Carbonated Hydroxyapatite, and Natural Calcium Carbonate: Relationship to Surface Energies, *J. Biomed. Mater. Res.* 1999; 45: 140–147.
 - 11 Detsch, R., Mayr, H., Ziegler, G. Formation of Osteoclast-Like Cells on HA and TCP Ceramics, *Acta Biomater.* 2008; 4: 139–148.
 - 12 Doi, Y., Koda, T., Wakamatsu, N. Influence of Carbonate on Sintering of Apatites, *J. Dent. Res.* 1993; 72: 1279–1284. Akatsu, T., Tamura, T., Takahashi, N. Preparation and Characterization of a Mouse Osteoclast-Like Multinucleated Cell Population, *J. Bone. Miner. Res.* 1992; 7: 1297–1306.
-